Graphene-based Filtration Media for Spacecraft Potable Water Systems: An Early Investigation

Rogelio E. Garcia Fernandez[1]
Jacobs Technology Inc., Houston, Texas, 77058

Michael Callahan[2]
NASA Johnson Space Center, Houston, TX, 77058, USA

and

Luke Gurtowski[3]
U.S. Army Engineer Research and Development Center, Vicksburg, Mississippi, 39180

Graphene-based materials have allowed fundamental advances in fields such as energy storage, electronics development, material science, optics, medicine, and water processing due to its unique two-dimensional structure, mechanical robustness, large surface, and high conductivity. However, little to no effort has been devoted to exploiting and studying these materials to develop new water technologies suited for spacecraft applications. One such application is the potential use of graphene-based materials as filtration media for reclaimed water. Therefore, studying the adsorptive performance of these new materials becomes crucial in identifying the opportunity to replace/upgrade State-of-the-Art filtration media currently used in space vehicles with water-recovery capability; especially if consumable requirements can be lessened as a result of extended filtration capacity. This early life-support-systems investigation pioneers in graphene-research by testing a number of graphene-based materials in comparative adsorption and antimicrobial experiments where contaminant removal efficiency, maximum adsorption capacity, and log reduction are probed. This preliminary investigation informs on the practicability of using graphene-based materials as filtration media and provides a discussion on the scaling-up and optimization of this prospective filtration technology for spacecraft potable water systems.

I. Nomenclature

$C_3H_8O_2$	=	propylene glycol
C_{ct}	=	specific contact-time concentration
C_e	=	equilibrium concentration
C_i	=	initial adsorbate concentration
GACT	=	graphene-based adsorption capacity test
GBF	=	Graphene-based Filtration
GBM	=	Graphene-based Materials
GNP	=	Graphene Nanoplatelets
IC	=	Ion Chromatography
ISS	=	International Space Station
K	=	isotherm or kinetics-based constant
MF	=	Multifiltration
$(NH_4)HCO_3$	=	ammonia bicarbonate
NH_4^+	=	ammonium ion
q	=	specific adsorption capacity
q_e	=	equilibrium adsorption capacity
q_{max}	=	maximum adsorption capacity
R^2	=	coefficient of determination
SOTA	=	State-Of-The-Art
SWRS	=	Spaceflight Water Recovery Systems
t	=	time
TIC	=	Total Inorganic Carbon
TOC	=	Total Organic Carbon
V	=	volume of the solution
WPA	=	Water Processor Assembly
η	=	removal efficiency

[1] Life Support Systems Test Engineer, JETS II Contract, Jacobs Engineering, 2224 Bay Area Blvd, Mail Stop: JE4EA.
[2] Water Technology Lead, Crew and Thermal Systems Division, 2101 E NASA Pkwy, Mail Stop: EC3.
[3] Research Chemical Engineer, Environmental Engineering Branch, 3909 Halls Ferry Rd, Mail Stop: Bldg. 3297.

I. Introduction

GRAPHENE is an one-carbon-atom-thick material first synthesized from graphite by Gem et al. in 2004 using the "scotch tape" method.[1] Figure 1 illustrates the structural difference between carbon, graphite, and graphene. The isolation of this two-dimensional material allowed the material science community to explore and probe the extraordinary properties of single layers of carbon atoms, and this effort led to the confirmation of graphene's exceptional electron mobility (200,000 cm^2/Vs)[2], supreme optical transparency (97.4%)[3], augmented thermal conductivity (3000-5000 Wm/K)[4], unprecedented mechanical strength (1.0 TPa)[5], and specific surface area (~2600 m^2/g).[6] The synthesis of stable mono-layer graphene permitted its reconfiguration into different Graphene-based Materials (GBM), such as graphene oxide, reduced graphene, functionalized graphene, graphene composites, graphene aerogels/hydrogels, and graphene-loaded materials. Graphene and GBM are thought to have a competitive adsorption capacity for a variety of water-stream contaminants. Various investigations have fundamentally studied the sorption performance of graphene and GBM for toxins[7], pharmaceuticals[8], water-soluble organics[9], volatile compounds[10], heavy metals[11], nuclear-waste contituents[12], oils[13], and dyes[14] reporting proficient contaminant-removal levels. Moreover, graphene and GBM gave been identified as potential materials for antimicrobial applications in water environments; nevertheless, microbial reduction by graphene has only been studied for a limited number of bacterial species, and clear physicochemical mechanisms have not been entirely developed to explain this reported antimicrobial property.[15–17]

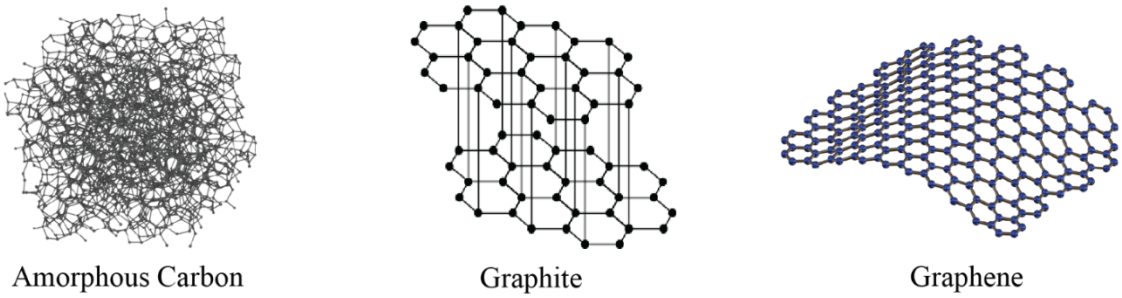

Figure 1. Structural Differences Between Amorphous Carbon, Graphite, and Graphene. *(Not to scale)*

Despite the advancements made in developing new materials and technologies using graphene and GBM, their physicochemical properties have been minimally studied in terms of their potential applications for water recovery and management in spacecraft life support systems. A keyword search for "graphene" in this conference's paper repository indicates that graphene-based technologies have only being considered for thermo-mechanical applications.[18] The promising adsorption performance of graphene across a wide range of water contaminants and its potential antimicrobial capacity has sparked interest in researching this material for water filtration purposes; specially, since tailored graphene-based filtration media could overcome limitations imposed by State-Of-The-Art (SOTA) spacecraft water technologies.

Currently, the Water Processor Assembly (WPA) aboard the International Space Station (ISS) is the SOTA process unit for Spaceflight Water Recovery Systems (SWRS). The WPA processes wastewater through a series of processing steps, such as phase separation, physical/chemical filtration, heating/cooling, oxidation, ion exchange, and disinfection. Matured graphene-based water technologies could improve such systems by serving as filtration media with higher removal capacity for organic and inorganic impurities, as well as microbial loads in some capacity. In the WPA, the majority of the water-soluble contaminants are removed by ion exchange and adsorption media contained in the Multifiltration (MF) beds, which constitute a significant mass requirement (~14.0 kg).[19] On the other hand, microbes present in the process water that manage to pass through the MF beds are primarily eliminated through a subsequent step of high-temperature oxidation. Following this step, a residual biocide is introduced to inhibit any microbial growth in the product water.[20] If Graphene-Based Filtration (GBF) media consist of single generalist adsorbent with better removal affinity towards microbes, ionic and nonionic organics and inorganics, future WPA-like units might be optimized for extended reliability and deployed for longer manned missions to the moon or mars. Consequently, in order to determine if there is a potential for improving water-filtration technologies, it is necessary

to conduct a trade study that compares the adsorptive and antimicrobial properties of graphene and GBM with SOTA filtration media.

Pristine graphene is theoretically regarded as an exceptional adsorbent for a variety of adsorbates due to its large natural surface area. Some studies have been able to produce graphene grades with high surface areas ranging between 2640-3355 m^2/g.[21,22] Since this material has an authentic two-dimensional structure and/or comprise of highly-accessible nanopores, most of its surface would be active/available for adsorption provided good-contact with the adsorbate-carrying phase. In contract, SOTA particles consist of spherical beads with macropores, mesopores, and micropores whose interior active surface is susceptible to diffusion-based transport limitations. This obstruction might limit the active surface area of SOTA filtration media. The WPA MF beds incorporate two engineered particles: AmberSorb® 4652 (~1400 m^2/g) for organic removal and AmberLite® IRN-150, IRN-77, IRA67 (~750 m^2/g) for removal of ionic inorganics. Despite the potential increase in active surface area resulting from its geometric conformation, graphene only comes in the form of nano powder/platelets, which are aggregates of graphene layers with a thickness of a few nanometers and a width of a couple of micrometers. Hence, available pristine graphene particles cannot be instantaneously consolidated into a flow-thought packed bed for testing since the minuscule powder will require high pressure for normal system flow rates. Nevertheless, the adsorption capacity of graphene for spacecraft-water contaminants has not yet been extensively studied by a Life Support System-focused research group, and this effort constitute an opportunity to develop the next generation filtration media for SWRS applications.

This early investigation intends to pioneer in graphene research by conducting a series of adsorption capacity tests with different grades of commercially-available graphene and GBM products. The Graphene-based Adsorption Capacity Tests (GACT) seeks to provide the necessary metrics to estimate the maximum (apparent) adsorption capacity of graphene and GBM for a selection of SWRS-related contaminants. The adsorption capacity (or loading) is the amount of adsorbate taken up by the adsorbent per unit mass (or volume) of the adsorbent. This parameter will be compared to the corresponding values for SOTA media. Furthermore, this effort will explore the in-house preparation of graphene-infused/enhanced filtration media by which adsorptive properties of graphene and the high water-permeability of porous materials are combined. The knowledge acquired thought this investigation will demonstrate the practicality of using graphene and GBM as SWRS filtration media and provide preliminary parametrization for the scaling up and optimization of graphene-based water technology.

II. Graphene-based Adsorption Capacity Tests

The GACT employed batch-mode experiments in which contaminated water is allowed to interact with a predetermined load of filtration media in mixing conditions for a specific contact-time duration. By measuring the contaminant (adsorbate) concentration at different contact times and adsorbent loads, isotherm diagrams for can be constructed to visualize the adsorption process at equilibrium. Similarly, the same measurments can be used to build an adsorption-kinetics diagram describing the transient characteristic of the apparent adsorption process. For both data-representation schemes, the specific adsorption capacity needs to be computed for a range of contact times and adsorbent loads at a fixed adsorbate loading; this metric is calculated as

$$q = \frac{(C_i - C_{ct})V}{m} \tag{1}$$

where C_i, C_{ct}, V, *and* m are the initial adsorbate concentration (mg/L), the adsorbate concentration (mg/L) at a specific contact-time, the volume of the solution (L), and the mass of the adsorbent (mg), respectively. Eq. 1 also computes the equilibrium adsorption capacity (q_e) when "C_{ct}" reaches a saturation point or equilibrium concentration (C_e). When q_e is plotted against C_e, the graph reveals an isotherm. On the other hand, one can visualize the adsorption kinetics of each experimental condition by plotting q vs. time (t, [min]). By building these plots, mathematical models can be deployed to fit the data and with the proper degree of regression, the corresponding maximum adsorption capacity (q_{max}) or the kinetic constant (K) can be determined from a theoretical basis. The GACT will utilize the adsorption models (and their linearized expressions) listed in *Table 1* to determine limiting adsorption pathways and the respective mathematical coefficients. In Addition, the experimental data will also determine the contaminant/adsorbate removal efficiency (η), which is computed using Eq. 2 and describes how much contaminant (%) has been removed at a discrete adsorbate concentration point.

$$\eta = \frac{C_i - C_{ct}}{C_i} \times 100\% \tag{2}$$

Table 1. Adsorption Models and Their Linearized Expressions

Adsorption Model	Expression	Linear Expression	Plot
Langmuir[23]	$q_e = q_m\left[\frac{K_L C_e}{1+K_L C_e}\right]$	$\frac{1}{q_e} = \left[\frac{1}{K_L q_m}\right]\left[\frac{1}{C_e}\right] + \frac{1}{q_m}$	$\frac{1}{q_e}\ vs.\ \frac{1}{C_e}$
Freundlich[24]	$q_e = K_F C_e^{1/n}$	$ln(q_e) = ln(K_f) + \frac{1}{n} ln(C_e)$	$ln(q_e)\ vs. ln(C_e)$
pseudo-1st order kinetic[25,26]	$q = q_e^{\left(1-e^{-K_1 t}\right)}$	$\ln(q_e - q) = -K_1 t + ln(q_e)$	$\ln(q_e - q)\ vs. t$
pseudo-2nd order kinetic[27]	$q = \frac{K_2 t q_e}{K_2 t + 1}$	$\frac{t}{q} = \left[\frac{1}{q_e}\right] t + \frac{1}{K_2 q_e^2}$	$\frac{t}{q}\ vs. t$
intraparticle diffusion[28,29]	$q = K_{id} t^{0.5}$	$q = K_{id} t^{0.5} + s$	$q\ vs. t^{0.5}$

s: thickness of the boundary layer

A. Test Methodology

The GACT collected experimental data based on a matrix of adsorbates and adsorbents. The adsorbates comprised of inorganics and/or organics found in ISS wastewater streams. To narrow down graphene's affinity to certain contaminants and to meticulously understand how the nature of the contaminant affect the adsorption process, single-component aqueous solutions were prepared to initiate the benchtop adsorption experiments. The main inorganic and organic contaminants consisted of ammonia bicarbonate ($(NH_4)HCO_3$) and propylene glycol ($C_3H_8O_2$), respectively. The reason for selecting these molecules as adsorbates is their association with the highest contaminant concentration in ISS reclaimed water[30], in addition, their solutions can be prepared easily and stored stably. Through out the GACT, the $(NH_4)HCO_3$ concentration was quantified based on the concentration of its respective cation via Ion Chromatography (IC) measurements. Contrarily, the concentration of $C_3H_8O_2$ was measured as Total Organic Carbon (TOC) via high temperature catalytic oxidation. Moreover, the GACT selection of adsorbates (Figure 2) was based on existing SOTA media inventory and in-stock grades of graphene. The GACT incorporated the following adsorbates: Graphene Nanoplatelets (GNP)*, granulated graphene†, UltraClean™ UCW 3600‡, and AmberSorb™ 4652.§

The adsorption experiments were carried in batch mode with moderate mixing mediated by magnetic stirring (Figure 4). Using sealed glass jars, the selected adsorbates and adsorbents were allowed to interact for a predestined contact time. The GACT testing matrix consisted of an array of increasing contact times, an array of varying adsorbate loads, and a fixed contaminant concentration. Each jar was assigned a contact time (5 min, 15 min, 30 min, 60 min) and accommodated enough volume for the extraction of quadruplicated samples. The adsorbate amount ranged from 50-800 mg.** Therefore, 0.2 L was added to each contact-time-assigned jar since this volume allowed the picked replication and the minimum volume required by the IC (10 mL) and TOC (40 mL) analyzers. When a contact time was reached, aliquots were withdrawn from the jar using a sterile syringe and transferred to a test tube after a filtration step using a 0.2 µm nylon filter. Since GNP generated well-dispersed suspensions that rapidly saturated syringe filters, the aliquots were placed in a centrifuge at 5000 revolutions per minute for five minutes. Then, the resulting supernatant was collected and filtered.

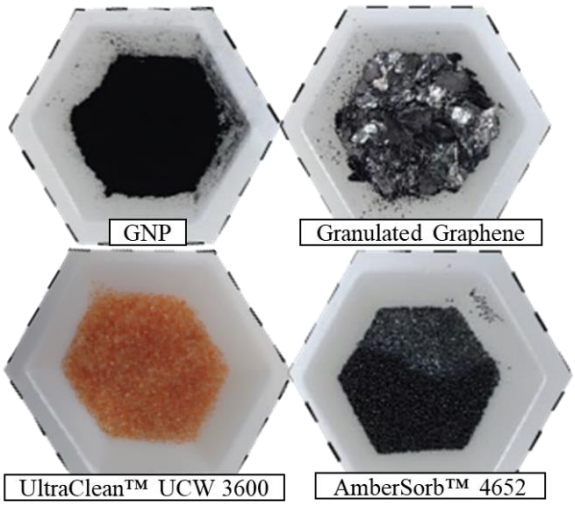

Figure 2. GACT Adsorbates

* xGnP® graphene nanoplatelets, 750 m^2/g produced by XG Sciences, Inc.
† Graphene Supermarket® Thermally Conductive Granulated Graphene.
‡ Formerly known as Purolite® NRW36; ion exchange resin for the (ACTEX) cartridge.
§ SOTA filtration media for the ISS MF beds produced by Dow Chemical Company.
** Higher loadings (up to 6400 mg) were tested, but η levels reached 100% before the 5-min contact time.

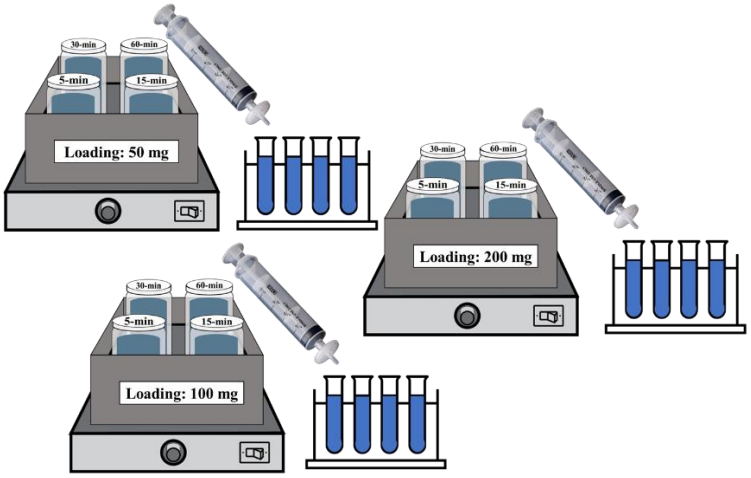

Figure 3. Graphene Adsorption Capacity Test

III. Results and Discussion

First, q and η values were calculated by analyzing the anticipated and inherent performance of the adsorbents in removing specific pollutants. For example, AmberSorb™ 4652 was not intentionally tested with $(NH_4)HCO_3$ solutions as its primary function does not involve the removal of inorganic substances like ammonium ion (NH_4^+) or Total Inorganic Carbon (TIC). By the same token, q and η metrics for the adsorption of organics by UltraClean™ UCW 3600 are not present in this section since the test matrix did not include experiments with this adsorbate and a $C_3H_8O_2$ solution. The initial concentration of the NH_4^+, TIC, and $C_3H_8O_2$ solutions were 100 mg/L, 90 mg/L and 6 mg/L (TOC), respectively. Figures 4, 5, and 6 summarized the results for the adsorption of NH_4^+, TIC, and TOC based on η values. It should be pointed out that first experiments with $C_3H_8O_2$ solutions did not provide a broad set of data at different material loadings, which was necessary to carry out the target data analysis. The interpretation of this outcome suggested that propylene glycol was not heavy enough for adsorption to occur a low concentration (6.0 mg/L). Consequently, 2-(2-Butoxyethoxy)Ethanol was selected as the new organic molecule for the single-component contaminate solution since it is one of the heaviest organic molecules found in ISS reclaimed water[30]. By selecting 2-(2-Butoxyethoxy)Ethanol a more responsive set of experimental data was collected at low (6.0 mg/L) and intermediate (40.0 mg/L) TOC concentrations.

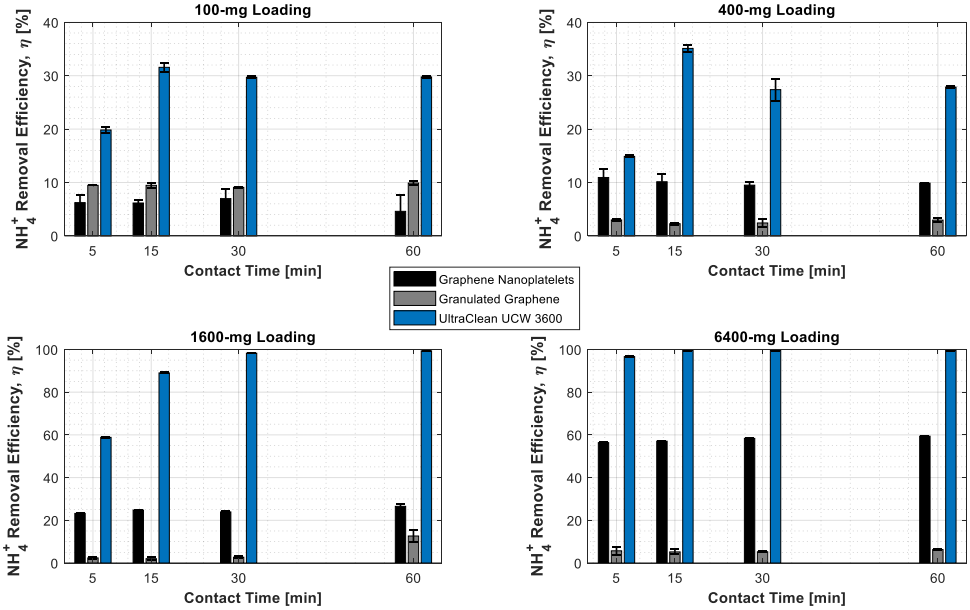

Figure 4. NH_4^+ Removal Efficiency vs. Contact Time at Different Adsorbate Loadings.

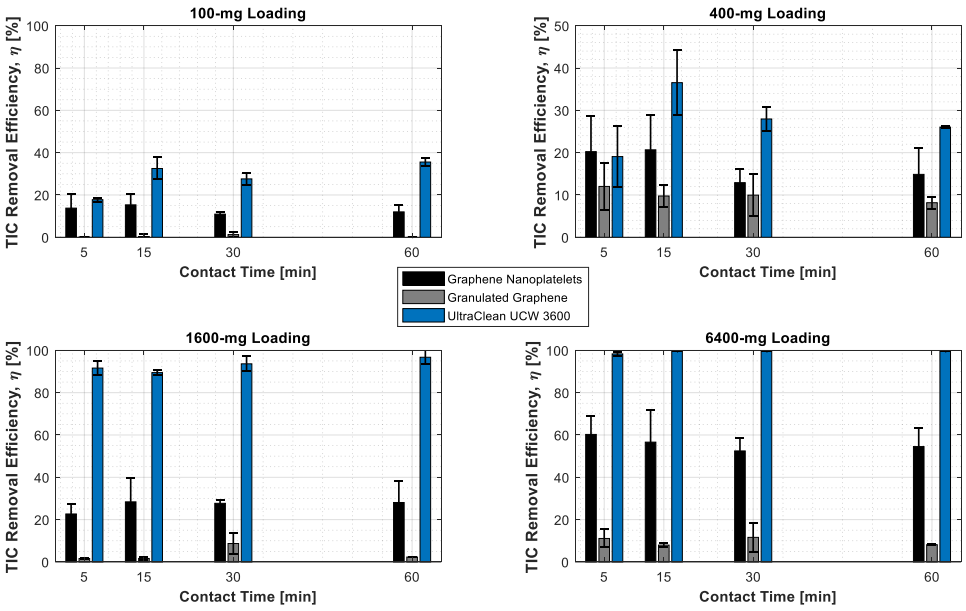

Figure 5. TIC Removal Efficiency vs. Contact Time at Different Adsorbates Loadings.

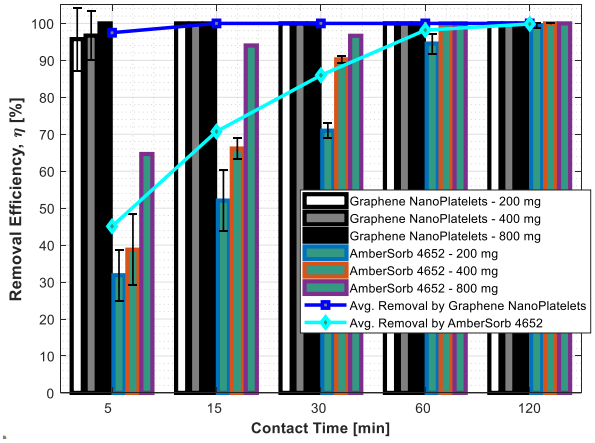

Figure 6. TOC [6.0 mg/L] Removal Efficiency vs. Contact Time at Different Loadings.

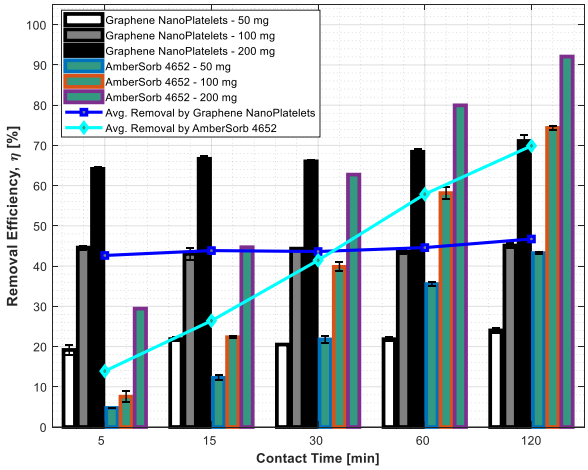

Figure 7. TOC [40.0 mg/L] Removal Efficiency vs. Contact Time at Different Loadings.

As expected, Figure 4 shows that the removal of NH_4^+ is enhanced as the adsorbate loading increases. Surprisingly, the 100-mg result in the same figure reveals that granulated graphene outpaced GNP in NH_4^+ removal by a few percents; however, this adsorbate does not response with higher removal percentages than GNP as loading increased. Granulated Graphene is made by rolling GNP to create larger pieces of graphene material; the surface area of the precursor GNP is unknow. Knowing the specific volume-to-material ratio at which the expensive GNP and the more affordable granulated graphene exhibit similar performance is beneficial, regardless of the aforementioned restriction. More significantly, Figure 4 demonstrates that the GBM did not surpass UltraClean™ UCW 3600 at any point. Note that Granulated Graphene loadings did not remove any TOC during the experiments. This SOTA adsorbate behaved nicely at removing more NH_4^+ as the loading increased. Note that the metrics for GNP in Figure 4 maintained a close η level at each contact time, and the charts did not capture an obvious transient phase. This trend, which is also seemed in Figure 5, might indicate that the GNP had reached its specific adsorption capacity for these loadings. Therefore, the selected contact-time resolution might have not been wide enough to fully capture a well-defined time-dependent correlation.

In a similar fashion, Figure 6 shows how quickly GNP removed all of the organic contaminant at each loading. Figure 6 compiles the η for GNP and AmberSorb™ 4652 at three different material loadings (note that the loading-based averaged results are also plotted). The result for GNP still constrained the q_{max} estimation since the metrics were not diverse enough for an isotherm or kinetics analysis. In contract, the same figure illustrates the desired removal trend with the performance of the SOTA adsorbent. Although AmberSorb™ 4652 provided dispersed metrics, these results were not further processed for theoretical parameter estimation since the corresponding GNP data was unsuitable for analysis. However, the ability of GNP to remove the same amount of TOC faster than the SOTA material is found to be compelling and attractive for certain applications. Furthermore, the concentration of the TOC was increased to 40.0 mg/L to resolve the undesired performance of GNP observed in Figure 6. Hence, the GACT was repeated with the new TOC level.

Figure 7 presents a set of results that are more suitable for isotherm and/or kinetics analysis since η values have a better distribution over the selected experimental conditions. Specifically, the GNP nor AmberSorb™ 4652 metrics reached the same level of removal at any material loading. While the longer contact-time points do not correspond to practical resident times for in-line configurations, the distribution of the data points is essential to determine scale-up parameters. This chart also informs that GNP still removes TOC faster than the SOTA adsorbate; however, it reaches a saturation point as quicker as well. Nevertheless, the adsorption of TOC by GNP was at least twice as higher as the TOC reduction permitted by AmberSorb™ 4652 at the earlier contact times. Below, the associated isotherm and kinetics diagrams for each adsorbate-contaminant combination are gathered. Note that only the adsorption models that provided the best fit are presented in this section. Figures 8, 9, 10 showcase the extensive adsorption modelling and the respective plots that fit the data, primarily for GNP.

The results for all adsorbates are summarized in Table 2. The adsorption of NH_4^+ and TIC by GNP was predominantly described by pSeudo-2nd Order Kinetics, with a 0.9999 and 0.9996 coefficient of determination (R^2), respectively. On the other hand, the adsorption process for same contaminants better fitted the Langmuir model when Granulated Graphene and UltraClean™ UCW 3600 were the adsorbents. However, the corresponding R^2 values were below 0.9. It is worth noting that Kinetics-based modelling offers more refence points since more than one adsorbate loadings can be simultaneously used to compare the regression characteristics. Contrarily, Isotherm-based modelling can only be carried out with the single array of data representing equilibrium points.

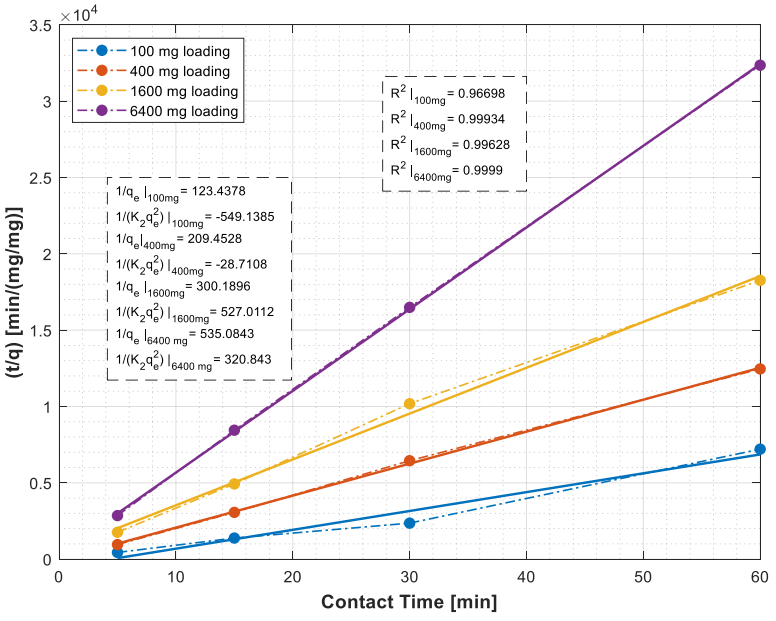

Figure 6. pSeudo-2nd Order Kinetics - NH_4^+ Adsorption by GNP.

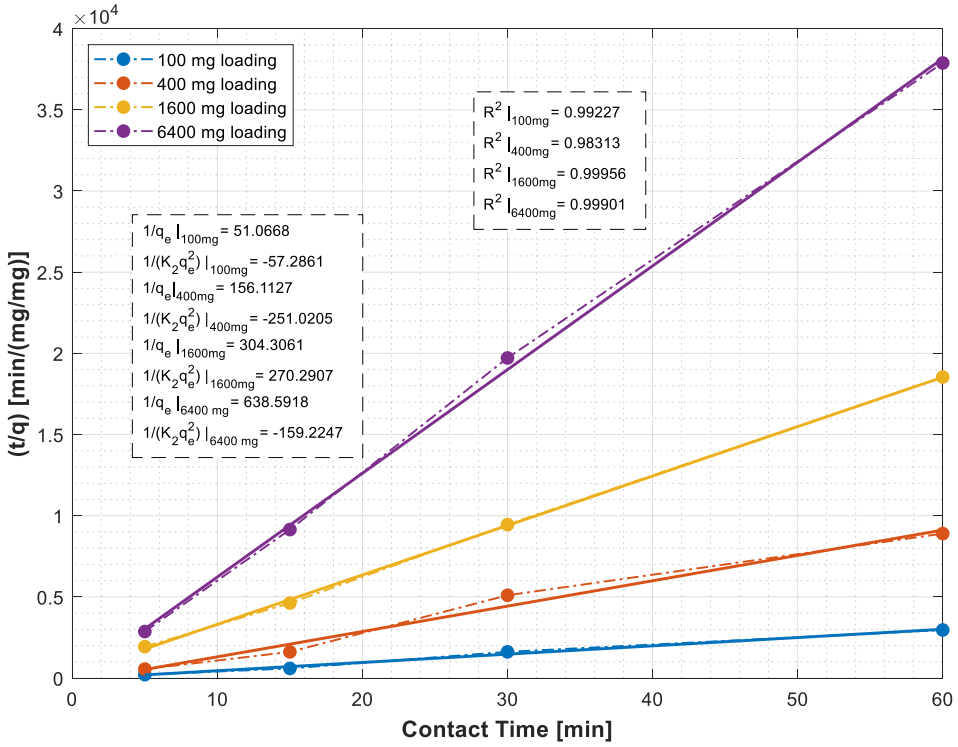

Figure 7. pSeudo-2nd Order Kinetics - TIC Adsorption by GNP.

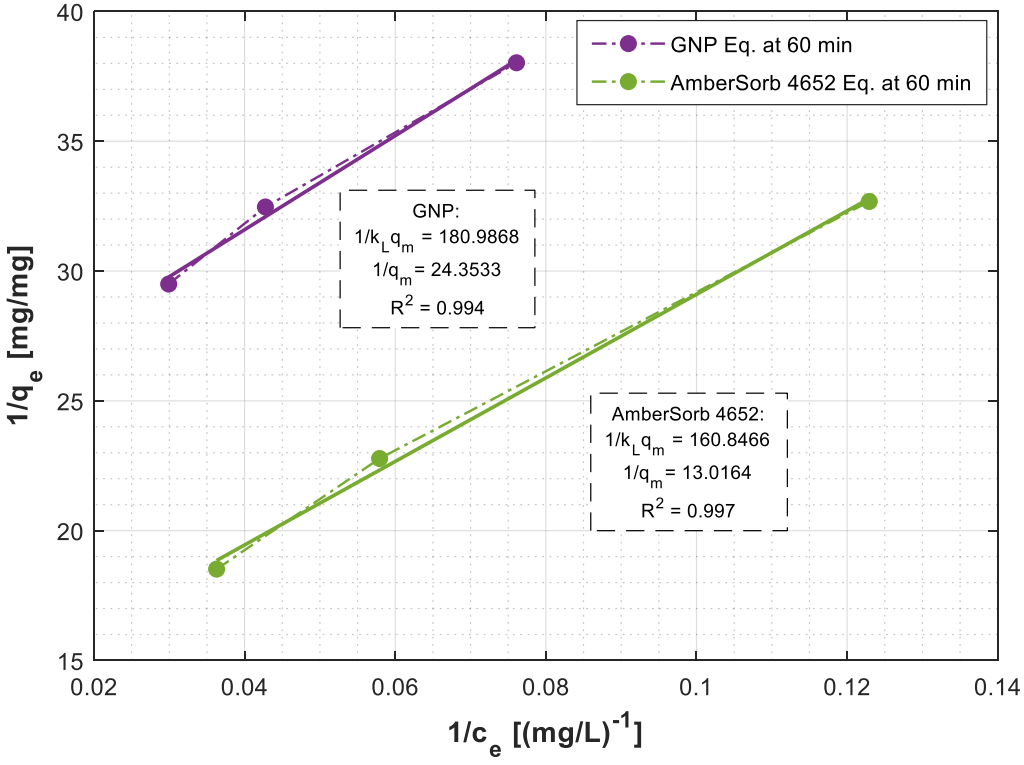

Figure 8. Langmuir-1 Isotherms - TOC Adsorption by GNP and AmberSorb™ 4652

Table 2. Isotherm & Kinetics-based Modelling Summary

Adsorbent	Adsorbate	Best-fit Model	R^2	Parameter	
				q_e [mg/mg]	K_2 [mg/(mg min)]
GNP	NH4+	Psudo-2nd Kinetics	0.9999	1.87×10^{-3}	$8.92 \times 10^{+2}$
GNP	TIC	Psudo-2nd Kinetics	0.9996	3.29×10^{-3}	$3.43 \times 10^{+2}$
||	||	||	||	q_{max} [mg/mg]	K_L [L/mg]
Granulated Graphene	NH4+	Langmuir	0.8177	1.22×10^{-3}	4.94×10^{-3}
Granulated Graphene	TIC	Langmuir	0.7002	5.51×10^{-4}	1.39×10^{-2}
UltraClean™ UCW 3600	NH4+	Langmuir	0.9484	2.69×10^{-2}	2.63×10^{-1}
UltraClean™ UCW 3600	TIC	Langmuir	0.9731	1.73×10^{-2}	3.99×10^{-1}
GNP	TOC	Langmuir	0.9940	4.11×10^{-2}	1.35×10^{-1}
AmberSorb™ 4652	TOC	Langmuir	0.9969	7.68×10^{-2}	8.09×10^{-2}

Moreover, during the regression analysis, the values of the slope and y-axis intercept needed to be carefully assessed. Most of the models in Table 1 predict a positive value for these parameters, with the exception to *pseudo-1st order kinetic* model. Therefore, regression coefficients were discarded when the values did not match the expected trend even if their respective R^2s were close to one. For instance, Figure 8 shows that the best-fit for NH_4^+ adsorption was provided by the 6400-mg loading experiment while Figure 9 indicates that TIC adsorption was best described by the 1600-mg experiment. These results reveal that GNP has a higher q_e for TIC than for NH_4+. Nevertheless, the corresponding K_2 values suggest that NH_4^+ adsorption might occur at a faster rate. Furthermore, Tablet 2 displays that the *Langmuir* model best fitted the data for the removal of inorganics mediated by Granulated Graphene and UltraClean™ UCW 3600. It is also important to point out that TOC removal by Granulated Graphene was not detect. The q_{max} values show that Granulated Graphene has less affinity for NH_4^+ and TIC than GNP. Note that modelling of Granulated Graphene-based data generated the worst regression levels. Whereas Granulated Graphene provided the lowest R^2 values, UltraClean™ UCW 3600 produced better regression and increased q_{max} to a magnitude higher than the q_e by GNP and Granulated Graphene. This result confirms the superiority of the SOTA adsorbent for the removal of ionic inorganics. It is to be noted that some linearized isotherms plots were omitted for brevity.

Figure 10 combines the linearized isotherms for GNP and AmberSorb™ 4652 solely for the removal of TOC. The plot also contains the values for the respective slope, y-axis intercepts, and R^2. The equilibrium points from the adsorption experiments at different loadings were selected from the 60-min contact-time point. Although samples at a 120-min contact time were collected, the processed data generated similar results. In other words, equilibrium was well defined by 60 minutes of contact time. Despite the statistical constraints imposed by the limited number of data points, Figure 10 shows an acceptable agreement with the linearized model. As it has been noted, certain GNP loadings removed TOC too quickly and/or the final TOC concentrations were under the limit of detection. Also, the available instrumentation does not confidently provide material-weight measurments below 50 mg. Table 2 substantiates that the TOC-based q_{max} for GNP is virtually half that of the SOTA adsorbent. In addition, the results reveals that the energy constant related to the heat of adsorption (K_L) is lower for AmberSorb™ 4652. Even though the modelling demonstrated that the SOTA adsorbent still performance better GNP, recall that GNP were tested in its pristine form without any precondition or engineering. This realization is remarkable and can provide the foundation for potential optimization paths for graphene-based filtration media. Nevertheless, these adsorption experiments need to be repeated with multi-component contaminant solutions or standardized solutions based on ISS ersatz wastewater stream.

Another important aspect of these results is the effects of nanoplatelet aggregation on the adsorption process. It is known that GNP easily stack on each other in water-based suspensions, and this mechanism reduces the active surface area of the material. Consequently, the performance of GNP might have been impacted by the lost of active surface are due to aggregation. Although this mechanism can be reduced by adjusting the acidity of the contaminant solution and reducing the GNP load, the experiments did not attempt adjusting the acidity of the associated solutions, and the lowest-possible measurable material loading still created saturated GNP suspensions. Futures studies will accommodate the necessary testing adjustments to reduce the impact of aggregation on the GACT.

IV. Conclusions

In conclusion, the research conducted by the Johnson Space Center Water Technology Development Group compared the performance of SOTA adsorbents with graphene and GBM in removing organic and inorganic contaminants from water. The results indicated that the UltraClean™ UCW 3600 outperformed GNP and Granulated Graphene in removing inorganic contaminants. However, GNP exhibited comparable performance to AmberSorb™ 4652 in removing TOC. This result is highly promising since GNP did not undergo any preconditioning or engineering process prior testing, and AmberSorb™ 4652 had a surface area per mass that was almost twice as large that of GNP. This comparison of metrics between these materials has established a relevant performance baseline for graphene and SOTA filtration media, and it opens up possibilities for further technological development. By understanding how graphene performs in its pristine form and comparing it with existing adsorbents, our group has a better understanding of how to identify potential paths for optimization, either through preconditions or integration with other particles. The isotherm and kinetics-based modelling has generated a matrix of parameters that can be deployed in geometry-based Multiphysics modelling for the design of realistic filtration components. The research team plans to further investigate the performance of graphene and GBM with multicomponent contaminant solutions and explore its integration with materials that have good water permeability (resins, foams, composites, etc.). By immobilizing GNP on other particles, the effects of nanoplatelet aggregation on adsorption can be prevented, and the high-pressure drops associated with fine particles can be dismissed. This work shows promising prospects for designing the next generation of filtration media for SWRS. The team's enthusiasm for this research is clear, and upcoming papers will present updates on graphene-loaded particles and the flow-through testing of GBF systems.

V. Acknowledgments

The authors would like to acknowledge and thank The National Aeronautics and Space Administration Center Innovation Fund for their interest and support to this research. Additionally, the Johnson Space Center Water Technology Development Group would like to express their appreciation to the U.S. Army Engineer Research and Development Center for their valuable collaboration on this project. Finally, the lead author's appreciation goes to Leopoldo Romero & Chirrs Carrier (JSC Water Analysis Lab), Ryan Dippolito (NASA Pathways Intern), Stacey Marshall and Dean Muirhead (JSC Water Technology De. GRP.) for their extensive contribution to the execution of this investigation.

References

[1] K.S. Novoselov, A.K. Geim, S.V. Morozov, D. Jiang, Y. Zhang, S.V. Dubonos, I.V. Grigorieva, and A.A. Firsov, "Electric Field Effect in Atomically Thin Carbon Films," Science **306**(5696), 666–669 (2004).

[2] Y. Zhang, T.-T. Tang, C. Girit, Z. Hao, M.C. Martin, A. Zettl, M.F. Crommie, Y.R. Shen, and F. Wang, "Direct observation of a widely tunable bandgap in bilayer graphene," Nature **459**(7248), 820–823 (2009).

[3] P. Blake, P.D. Brimicombe, R.R. Nair, T.J. Booth, D. Jiang, F. Schedin, L.A. Ponomarenko, S.V. Morozov, H.F. Gleeson, and E.W. Hill, "Graphene-based liquid crystal device," Nano Letters **8**(6), 1704–1708 (2008).

[4] A.A. Balandin, S. Ghosh, W. Bao, I. Calizo, D. Teweldebrhan, F. Miao, and C.N. Lau, "Superior thermal conductivity of single-layer graphene," Nano Letters **8**(3), 902–907 (2008).

[5] T.J. Booth, P. Blake, R.R. Nair, D. Jiang, E.W. Hill, U. Bangert, A. Bleloch, M. Gass, K.S. Novoselov, and M.I. Katsnelson, "Macroscopic graphene membranes and their extraordinary stiffness," Nano Letters **8**(8), 2442–2446 (2008).

[6] F. Schedin, A.K. Geim, S.V. Morozov, E.W. Hill, P. Blake, M.I. Katsnelson, and K.S. Novoselov, "Detection of individual gas molecules adsorbed on graphene," Nature Materials **6**(9), 652–655 (2007).

[7] S.G. Zetterholm, L. Gurtowski, J.L. Roberts, S. McLeod, B.M. Fernando, and C.S. Griggs, "Graphene-Mediated removal of Microcystin-LR in chitosan/graphene composites for treatment of harmful algal blooms," Chemosphere **300**, 134583 (2022).

[8] L.A. Al-Khateeb, S. Almotiry, and M.A. Salam, "Adsorption of pharmaceutical pollutants onto graphene nanoplatelets," Chemical Engineering Journal **248**, 191–199 (2014).

[9] P. Lazar, F. Karlický, P. Jurecka, M. Kocman, E. Otyepková, K. Šafářová, and M. Otyepka, "Adsorption of small organic molecules on graphene," Journal of the American Chemical Society **135**(16), 6372–6377 (2013).

[10] V. Kumar, Y.S. Lee, J.W. Shin, K.H. Kim, D. Kukkar, and Y.F. Tsang, "Potential applications of graphene-based nanomaterials as adsorbent for removal of volatile organic compounds," Environment International **135**, 105356 (2020).

[11] M. Sivakumar, J. Widakdo, W.S. Hung, C.F. Wang, C.C. Hu, K.R. Lee, and J.Y. Lai, "Porous graphene nanoplatelets encompassed with nitrogen and sulfur group for heavy metal ions removal of adsorption and desorption from single or mixed aqueous solution," Separation and Purification Technology **288**, 120485 (2022).

[12] A. Yang, P. Yang, and C.P. Huang, "Preparation of graphene oxide–chitosan composite and adsorption performance for uranium," Journal of Radioanalytical and Nuclear Chemistry **313**(2), 371–378 (2017).

[13] V. Brancato, E. Piperopoulos, E. Mastronardo, L. Calabrese, C. Milone, and E. Proverbio, "Synthesis and Characterization of Graphite Composite Foams for Oil Spill Recovery Application," Journal of Composites Science **4**(4), 154 (2020).

[14] M. Abolhassani, C.S. Griggs, L.A. Gurtowski, J.A. Mattei-Sosa, M. Nevins, V.F. Medina, T.A. Morgan, and L.F. Greenlee, "Scalable Chitosan-Graphene Oxide Membranes: The Effect of GO Size on Properties and Cross-Flow Filtration Performance," ACS Omega **2**(12), 8751–8759 (2017).

[15] B. Omran, and K.H. Baek, "Graphene-derived antibacterial nanocomposites for water disinfection: Current and future perspectives," Environmental Pollution **298**, 118836 (2022).

[16] H. Ji, H. Sun, and X. Qu, "Antibacterial applications of graphene-based nanomaterials: Recent achievements and challenges," Advanced Drug Delivery Reviews **105**, 176–189 (2016).

[17] H. Zhou, F. Zou, K. Koh, and J. Lee, "Antibacterial Activity of Graphene-Based Nanomaterials," Advances in Experimental Medicine and Biology **1351**, 233–250 (2022).

[18] M. Molina, in (46th International Conference on Environmental Systems, 2016).

[19] M.J. Kayatin, D.L. Carter, R.G. Schunk, and J.M. Pruitt, in *International Conference on Environmental Systems* (2016).

[20] J. Williamson, A. Gleich, and J. Wilson, "Status of ISS Water Management and Recovery," (2022).

[21] P. Kamedulski, M. Skorupska, P. Binkowski, W. Arendarska, A. Ilnicka, and J.P. Lukaszewicz, "High surface area micro-mesoporous graphene for electrochemical applications," Scientific Reports **11**(1), 22054 (2021).

[22] L. Zhang, F. Zhang, X. Yang, G. Long, Y. Wu, T. Zhang, K. Leng, Y. Huang, Y. Ma, and A. Yu, "Porous 3D graphene-based bulk materials with exceptional high surface area and excellent conductivity for supercapacitors," Scientific Reports **3**(1), 1408 (2013).

[23] I. Langmuir, "The adsorption of gases on plane surfaces of glass, mica and platinum.," Journal of the American Chemical Society **40**(9), 1361–1403 (1918).

[24] H. Freundlich, "Over the adsorption in solution," J. Phys. Chem **57**(385471), 1100–1107 (1906).

[25] S.K. Lagergren, "About the theory of so-called adsorption of soluble substances," Sven. Vetenskapsakad. Handingarl **24**, 1–39 (1898).

[26] H. Yuh-Shan, "Citation review of Lagergren kinetic rate equation on adsorption reactions," Scientometrics **59**(1), 171–177 (2004).

[27] Y.-S. Ho, and G. McKay, "Pseudo-second order model for sorption processes," Process Biochemistry **34**(5), 451–465 (1999).

[28] V. Fierro, V. Torné-Fernández, D. Montané, and A. Celzard, "Adsorption of phenol onto activated carbons having different textural and surface properties," Microporous and Mesoporous Materials **111**(1–3), 276–284 (2008).

[29] W.J. Weber Jr, and J.C. Morris, "Kinetics of adsorption on carbon from solution," Journal of the Sanitary Engineering Division **89**(2), 31–59 (1963).

[30] D. Muirhead, S. Moller, N. Adam, and M. Callahan, "A Review of Baseline Assumptions and Ersatz Waste Streams for Partial Gravity Habitats and Orbiting Microgravity Habitats," (2022).